Control and Cybernetics

vol. **40** (2011) No. 1

Automatic north-wise alignment of sector sonar image* †

by

M. Borawski

Faculty of Computer Science and Information Systems
West Pomeranian University of Technology
ul. Żołnierska 49, 70-210 Szczecin, Poland
e-mail: mborawski@wi.ps.pl

Abstract: The paper discusses a method of north-wise alignment of sonar image adopted when it is located near the quay. In such a case, the built-in sonar's compass is prone to erroneous indication due to the influence of metal parts of the quay. The method is based on the determination of direction coefficient of the water line. Additionally, it allows for defining the maximal error caused by non-linearity of the quay, mutual blocking out by its different parts, and multiple reflection of acoustic echo.

Keywords: mosaic, sector-scan sonar.

1. Introduction

Sector sonar is a device used for recording the images at the sea or river floor, and objects located under water. Depending on the application, it can be hull-mounted or deployed in water (e.g. at the bottom). Hull-mounted sonars for non-military purposes are used mainly in fishing, and operate in frequency band of 60-80 kHz. High resolution sonars with frequency operating in the range 600kHz-2.3MHz are used for underwater inspections of rivers, hydro-technical construction and supervision of underwater works. These sonars have much greater resolution, but shorter range.

Characteristics of the sector sonar image are similar to the characteristics of the side sonar image. This results from the fact that both operate in approximately the same frequency bands and the principle of image formation is very similar. Consequently, many algorithms developed for side sonars can be used for sector sonars. Due to limited availability of data from sector sonars and high similarity of images from sector and side sonars, there is a limited number of publications devoted to specific aspects of sector sonar data processing. Most of

*Submitted: July 2010; Accepted: January 2011.

†This is an extended and amended version of the paper, presented at the 5$^{\text{th}}$ Congress of Young IT Scientists (Międzyzdroje, 23-25.IX.2010).

research on object recognition from sector sonar images focused on the selection of method most suitable for specific features of such images (Ruiz, Lane and Chantler, 1999), detection and identification of small objects (Perry and Guan, 2004a,b), detection and determination of the movement parameters of moving objects (Chantler and Stoner, 1994; Lane, Chantler and Dai, 1998).

Sonar image is recorded sequentially, line after line, no matter whether they are parallel or not. In the case of side sonar, it moves together with ship, approximately along straight lines. In sector sonar, after recording each line, the sonar's head is slightly rotated. In order to present the recorded objects in a correct way, it is necessary to relocate all the lines in conformance with their orientation in the real world and fill the gaps between them by means of interpolation. Image created in such a way is called a mosaic.

In the case of underwater inspection of hydro-technical structures, sector sonar is located in different positions at the bottom. This makes it particularly difficult to compose the mosaic. The most important problem is the availability of the (approximate) geographical coordinates of sonar locations. Similar problem arises for the side sonar located on the AUV (Autonomous Underwater Vehicle), see Reed et al. (2006). What is specific for sector sonar is that individual recordings have the same error of determining the geographical coordinates, while in the side sonar the error is related to individual lines.

Data of the sector sonar image contain in graphical file information about head angles, range, geographical position and azimuth, measured by built-in compass. If there is one location, such data are sufficient for making a mosaic. But if there are different locations, it is difficult to create a mosaic because of errors in geographical position. Geographical position is measured in respect to a ship or shore, and sonar is located at the bottom. As a result, there is a several-meter difference between the actual and estimated position. This difference can be even greater due to the movements of the sonar caused by the stream or bottom slope. Because the recorded images overlap partially, their registration is possible, e.g. owing to 2D correlation between the overlapping parts of images.

The adjustment of sector scan sonar's images facilitates the qualification of an image orientation in relation to the North. Unfortunately, in the case of registration near the pier, the operation of built-in compass can be deteriorated, most probably by the steel parts used for quay construction. Azimuth error can be serious, as illustrated in Fig. 1. In the extreme cases, it can amount to up to 40 degrees. Such a major error in image orientation makes it difficult to adjust images from different registrations. Taking a small distance from the quay into account, compass readings can be compensated on the basis of information about the quay location that is derived from the map. Software used for creating the mosaic usually aligns the mosaic in respect to the map under the assumption that the geographical location of quay is known. The paper presents the method for determining the orientation of sector sonar image in relation to the North, when the sonar is located close to the quay.

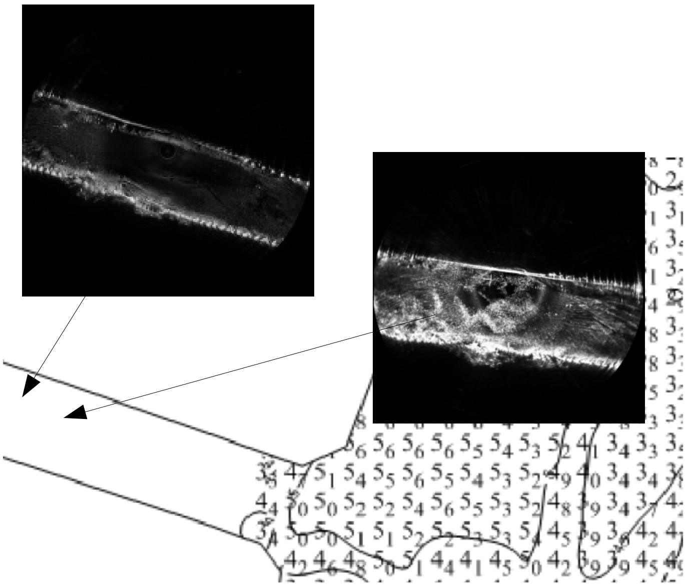

Figure 1. Map and sector sonar image of a channel (data source: Hydrograf XXI, Marine Academy of Szczecin)

The article also discusses the way of calculating the error of specified orientation. This error is important while comparing the images. It shows the range over which the compared images should be rotated. Calculating this error requires the set of vectors to satisfy the axioms of the Abelian group. In this case, it is not plausible to use fuzzy arithmetic for calculations. In the fuzzy arithmetic, researchers attempted to assure its conformity with the axioms of the aforementioned group, see e.g. Mareš (1977, 1989). He used decomposition as fuzzy numbers and then adopted convolution as addition, and finally created convolution representation. Nevertheless, a certain problem arises, namely this is not in accordance with fuzzy arithmetic. As a result, the definition of a set of fuzzy numbers is provided (the definition of the opposite element is in line with fuzzy arithmetic but not with the axioms of the group, Mareš, 1994). Similarly, there is a problem with classifying other sets of numbers that satisfy Abelian group axioms (e.g. directed fuzzy numbers proposed in Kosiński and Prokopowicz, 2004) into fuzzy arithmetic.

To make calculations, it is possible to use interval arithmetic, proposed by Kaucher (1973, 1980). By definition, it satisfies all the axioms of the Abelian group. Therefore, it can be employed for defining vectors in vector spaces. It requires one to assume that elements opposite to intervals do not necessarily have a physical representation, as suggested by Mikusiński in the operator calculus (Mikusiński, 1953, 1983).

2. Determination of azimuth

Determination of sector sonar image azimuth can be divided into the following stages:

1. Determination of quay segment,
2. Vectorization,
3. Determination of direction coefficient of straight line representing the quay line.

In order to determine the azimuth of the sector sonar image, it is necessary to detect the quay line. Because the sought value is an angle of the line formed by the quay, it is not essential to determine the line along which the quay meets the bottom or the waterline. Both lines have the same direction but differ in position shown by the sonar, which is not important here. The shape of the line illustrating the contact of the quay with the bottom depends on the depth and thus can have a very irregular shape. The line illustrating the contact of the quay with the water surface is more regular than the aforementioned one. Acoustic wave approaching from the water surface is strongly scattered and the area over the surface in most cases lacks acoustic echo. In sonar image it is shown as black colored area.

Materials used for quay construction can vary and their acoustic echo is practically always recorded by the sonar. Exclusion can be a quay with openings or extending parts, partially shadowing the quay. Shadowed or not visible areas form the acoustic shadow, i.e. space lacking the acoustic echo. In the case of a quay, acoustic shadow areas are normally the small parts of sonar image and are practically disconnected from the water line. To create such a situation, the shadowing object should be under the water, just over the sonar, or in its direct vicinity. Yet, this is very unlikely because there is a risk of sonar damage sounding is avoided in such places.

The literature discusses a number of methods for detecting the line. One of the most popular is the Hough transform or its modifications (Aggarwal and Karl, 2006; Ran and Chen, 2003). In this case, it is not difficult to detect the line as it can be read from the map. It is not very important to know its location, but its direction and uncertainty in its routing is necessary to determine the estimate of direction error. Thus, it is not essential to use the methods for line detection, but the vectorization of line and approximate determination of its origin and end.

The fact that the water line separates bright area from dark area can be used for determining its direction. When the sonar image is correctly recorded, its intensity range can be divided into three parts: acoustic shadow area, bottom area and area of strongly reflecting objects. If the amplification of sonar signal is very high (as is shown in Fig. 2), then the respective areas are easily discernible, using the intensity histogram. They form three local maxima. As the threshold value between acoustic shadow and the bottom, the local minimum between the intensity values in the shadow area and bottom area can be adopted.

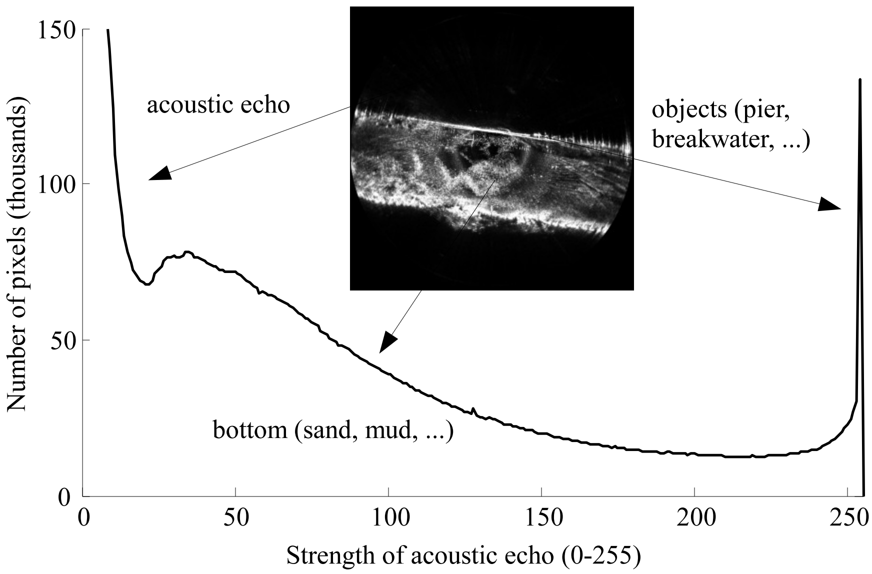

Figure 2. Histogram of sonar image

It is possible to find the acoustic shadow on the basis of local histogram minima, yet only for high resolution sonars using A/D converter of word length of 10 and more bits, or using high amplification of signal fed to the converter. If the amplification is too low, no minimum is found between the area of acoustic shadow and the bottom. The threshold separating the area of acoustic shadow should be determined experimentally for various amplifications and selected in line with the amplification used by sonar operator. Each change of sonar parameters is recorded in the sonar data file, allowing to read the set amplification level.

Fig. 3 presents the separated area of acoustic shadow. In order to decrease the noise level, at first the sonar image has been low-pass filtered with the use of averaging convolution mask of size 5x5. Next, the threshold of the value of 21 was selected, based on the histogram. For the sonar images with similar values of amplification, this is the correct value to be used for determining the acoustic shadow area.

Theoretically, the acoustic shadow area should have zero values of acoustic echo. But it is not true in practice because the sonar could record, instead of the lack of echo, multiple reflections from other parts of the bottom. As a result, the acoustic shadow area extends to echo intensity values representing the bottom. Thresholding allows to select the parts of the bottom not belonging to the area of acoustic shadow. However, this is not a serious problem as they do not belong to the area of acoustic shadow representing areas over the waterline.

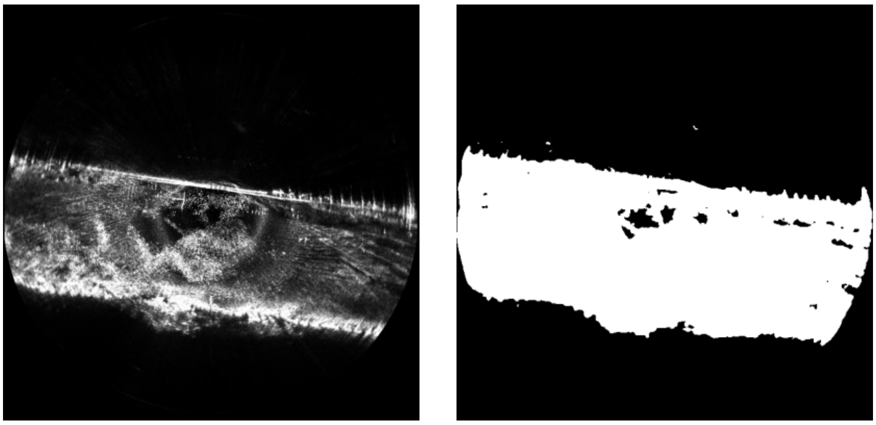

Figure 3. Sonar image of the channel and the separated acoustic shadow area (black)

Between the bottom and waterline there is the quay area for which the intensity of acoustic echo is always greater than the intensities for bottom echo.

After delimiting the border between the bright and dark areas, pixels should be changed into the coordinates of points. In principle, any method of vectorization can be used to do so. As for the solution under discussion, the method involves searching for consecutive border points based on the movement direction. First, the image is scanned line by line, from left to right, looking for non-zero point. The left vertical border and upper horizontal line are determined for this point. Coordinates of the borders are recorded. Then, the border is looked for to the right, in respect to the previous one, and three options are obtained. This is illustrated in Fig. 4. After selecting the border, it is recorded and another one is selected using the same principle, but a different method for searching the direction. Once the border has met the already recorded coordinates, the vectorization process is regarded as completed.

This vectorization method works for vectorizing a single object. In this case, there are many objects, and only the first one will be vectorized. To avoid such a situation, once vectorized, the first object is removed and replaced with zero values. Arbitrary method of polygon filling can be used for this purpose. The filling method by consistency, also known as the seeding algorithm, was employed. After removing the object, the vectorization process is repeated and each new detected contour is recorded in a separate table.

Additional white areas, forming excessive contours, are relatively small. One should select the biggest contour corresponding to the waterline. The coordinates of all points belonging to the border of sounding space are rejected. They are located on the circle. The circle and the image have a common centre. After rejecting these points, one line remains, in the case of sounding in the big river or big water reservoirs, or two lines in the case of sounding in channels. This is illustrated in Fig. 5. As for channels, if the approximate position of sonar is known, the identification of quay in the sonar image, for which the waterline is determined, can be made on the basis of distance from the center of the image to the recorded points of both lines.

The determination of sonar image azimuth requires the estimation of direction coefficient of the straight line $y = ax + b$, being the approximation of contour's points. This coefficient can be estimated using the least squares method, and the formula (Aczel, 2000):

$$a = \frac{\sum_{i=1}^{n} (x_i - \mu_x)(y_i - \mu_y)}{\sum_{i=1}^{n} (x_i - \mu_x)^2}\,, \tag{1}$$

where x_i and y_i are the coordinates of quay contour's points, n is the number of points, a is the estimated straight line direction coefficient, μ_x, μ_y are mean values of x_i and y_i series, respectively.

In order to determine sonar image azimuth, it is not necessary to estimate parameter b. Fig. 6 presents the quay line with overlaid straight line approximation (broken line). Direction coefficient enables determination of the angle in relation to the horizontal line. In the case under consideration, the angle equals 8 degrees. The azimuth angle (in the sonar images under discussion, it is at the top) equals 278 degrees. As the map suggests, it should be actually equal 290.5 degrees. This allows to correct the azimuth of sonar image. The image should be rotated by 12.5 degrees.

The fact that direction coefficient allows to determine the angle in the range from -90 to 90 degrees can pose a certain problem while determining the azimuth. A proper determination of the angle requires checking which side of the line contains the image of the bottom. This can be established by comparing the mean values of acoustic echo intensities, on both sides of the line. It is plausible to identify the position of the bottom relative to the line by comparing it with the map, which enables one to determine the angle in the full range.

Fig. 7 presents the line determined for another fragment of the quay, for different parameters of sonar operation. Based on the histogram, the selected threshold is 11. The angle determined in relation to the horizon is 10 degrees, and 280 relative to the North. Thus, the sonar image should be corrected by 10.5 degrees.

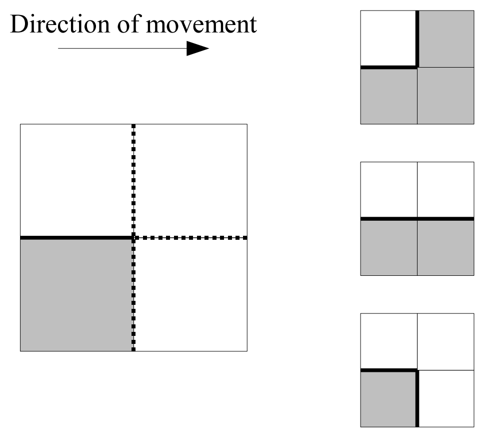

Figure 4. Object search direction during vectorization

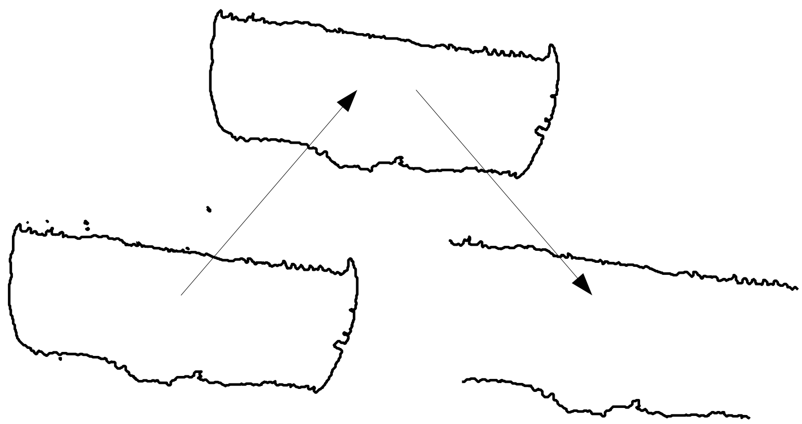

Figure 5. Sonar image after vectorization

Figure 6. Approximation of the line

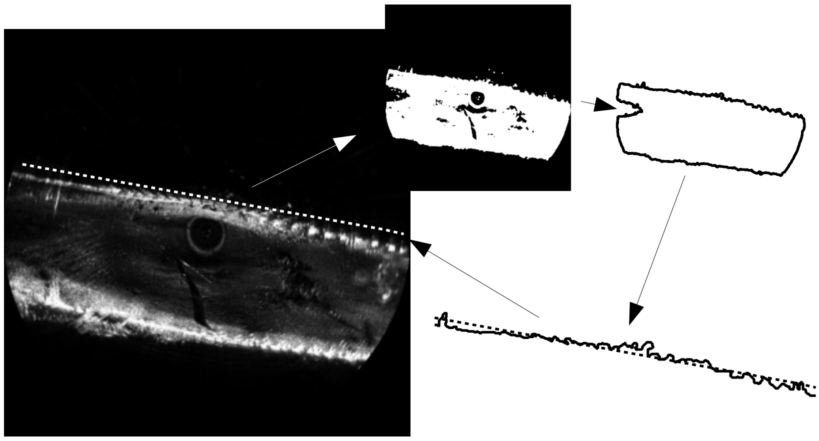

Figure 7. Determined line of the quay (data source: Hydrograf XXI, Maritime Academy in Szczecin)

3. Estimation of calculation of the angle error

Sonar image azimuth is determined with a certain error. It is related to the fact that the quay is not always constructed along ideal straight line, some parts of the quay are shadowing its other parts, and there are errors caused by multiple reflections of acoustic echo. The estimation of angle error is particularly important to the creation of mosaic from sector sonar images. Sonar images should be compared after angle correction. In image comparison methods, the same angle should be adopted. If the angle is subject to change, multiple comparison introducing incremental changes of the angle for one of the images can be made. If the possible range of difference between angles is known, the number of comparisons is limited.

Some indicator of the angle error calculation level is the maximal difference between the actual values y_i and those values obtained from the approximation $\hat{y}_i$:

$$\epsilon = \max_i |y_i - \hat{y}_i| \ . \tag{2}$$

Value ϵ determines the ranges containing the actual values y_i for specific x_i:

$$\forall x_i : y_i \in [\hat{y}_i - \epsilon, \hat{y}_i + \epsilon] \ . \tag{3}$$

For the sake of simplification, it was assumed that ϵ is the same for values over the axis and below the line determined by points $\hat{y}$. $[\hat{y}_i - \epsilon, \hat{y}_i + \epsilon]$ is an interval as defined by interval arithmetic. By substituting the intervals with values y_i in the formula (1) one obtains the interval containing direction coefficient a. It is assumed that values x_i are known, but values y_i allow for a

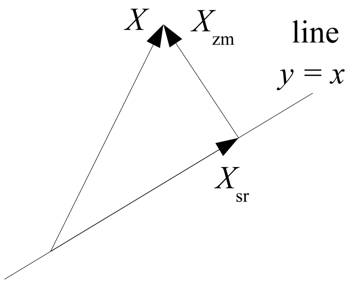

Figure 8. Division of vector X into vector representing the mean value X_{sr} and vector representing the variable component X_{zm} of vector X

certain error. Error relating to x_i is in this way transferred into the values of y_i. With such an assumption and with constant value of ϵ, the left bound of the range determining the value of direction coefficient a will always equal the right bound.

The fact that left and right bounds are equal for the direction coefficient can be easily justified with the interpretation of the formula (1) in vector space. Vector can be resolved into two vectors: vector representing the constant component X_{sr} and vector representing the variable component X_{zm} of vector X (Fig. 8). The coordinates of vector X_{sr} are calculated as the mean value of coordinates of vector X. All the coordinates of vector X_{sr} take the same value. On the other hand, vector X_{zm} is calculated as the difference between vectors X and X_{sr}. These vectors are always orthogonal (Borawski, 2007). The formula (1) is in fact used for calculating the vector component defined by coordinates $y_i - \mu_y$ along the vector determined by coordinates $x_i - \mu_x$ in the n-dimensional space. Due to the subtraction of mean value, vector representing the variable component will amount to zero. Projection on such a vector will never take into account the mean value of vector X, and thus the formula (1) will be identical with the formula:

$$a = \frac{\sum_{i=1}^{n} (x_i - \mu_x)\, y_i}{\sum_{i=1}^{n} (x_i - \mu_x)^2} \,. \tag{4}$$

Similarly, the projection of vector without constant component will have zero component along the constant component of any vector, thus the above formula will be identical with the following formula:

$$a = \frac{\sum_{i=1}^{n} x_i \left(y_i - \mu_y\right)}{\sum_{i=1}^{n} x_i^2} \ , \tag{5}$$

For real numbers the formulas (1), (4), and (5) will always give the same result.

In the case of interval arithmetic, values y_i will be replaced with intervals for which subtraction may be defined as follows (Neumaier, 1990):

$$\forall a, b \in \mathbb{IR} : a - b \equiv \left[\underline{a} - \bar{b}; \bar{a} - \underline{b}\right] \ , \tag{6}$$

where $\mathbb{IR}$ is the set of all intervals, $\underline{a}$, $\underline{b}$ are the left, and $\bar{a}$, $\bar{b}$ are the right bounds of intervals.

The subtraction of mean value in the numerator of the formula (1) will involve the following steps: the mean value of the left bounds of intervals will be subtracted from the right bounds of intervals, and vice versa - the mean value of the right bounds of intervals will be subtracted from the left bounds of intervals. In this way, mean value will not be removed completely. This value is responsible for the error of direction coefficient a. But the fact that it has not been removed has no influence, because the formula (1) is identical with the formula (4). Moreover, because vector $x_i - \mu_x$ does not contain mean value, and the error has only the mean value, it will not be taken into account in the calculation of direction coefficient a. Consequently, the interval for this coefficient will have zero width.

The result cannot be considered correct because the change in even one value y_i will have an impact on the value of directional coefficient a. Incorrect result is obtained via employing the interval arithmetic in the formula developed in line with vector calculus, which assumes operations on relative numbers. Relativity has to be complete, i.e. negative values of all possible parameters describing the number are allowed. In the case of interval arithmetic, one of the parameters cannot be negative. This parameter is the range of the interval.

Instead of interval arithmetic, extended interval arithmetic can be used for the calculation of the error range of direction coefficient values a. Moreover, for this purpose, only definitions of the addition operation (Kaucher, 1980):

$$\forall a, b \in \mathbb{H} : a + b \equiv \left[\underline{a} + \underline{b}; \bar{a} + \bar{b}\right] \ , \tag{7}$$

multiplication of the interval by the number not being an interval:

$$\forall \alpha \in \mathbb{R}, b \in \mathbb{H} : \alpha b \equiv \left[\alpha \underline{b}; \alpha \bar{b}\right] \ , \tag{8}$$

and the method for obtaining the opposite element, Popova (1994):

$$\forall a \in \mathbb{H} : -a \equiv \overline{[\underline{a}; \bar{a}]} = [-\underline{a}; -\bar{a}] \ , \tag{9}$$

where $\mathbb{H}$ is the set of all intervals in the extended interval arithmetic, including as a subset the set $\mathbb{IR}$, are required.

To enable the application of extended interval arithmetic for evaluating the straight line direction coefficient error, based on the formula (1), it is necessary to consider interval parts of vector space. The main condition is that the set of intervals $\mathbb{H}$, together with the operation of addition, defined by the formula (7) be the Abelian group. Upon defining the opposite element in accordance with the formula (9), it can be noticed all the axioms of the Abelian group are satisfied.

Based on the set of intervals, the ordered n-tuples can be defined:

$$\forall a_1, a_2, \ldots, a_n \in \mathbb{H}, B \in \mathrm{X} : B \equiv (a_1, a_2, \ldots, a_n) \ , \tag{10}$$

where X is the set of all vectors.

Set of all n-tuples with the addition operation can be defined as follows:

$$\forall A, B \in \mathrm{X} : A + B \equiv (a_1 + b_1, a_2 + b_2, \ldots, a_n + b_n) \ , \tag{11}$$

and it also forms the Abelian group.

The set X could be a set of vectors if the operation of multiplication by scalar is defined, and all the axioms of vector space are satisfied. Based on the formula (8) the operation of vector multiplication by the scalar can be defined as follows:

$$\forall a \in \mathbb{R}, B \in \mathrm{X} : aB \equiv (ab_1, ab_2, \ldots, ab_n) \ . \tag{12}$$

The set X and the aforementioned multiplication of vector by scalar satisfy all the axioms of vector space, thus the elements of this set can be interpreted as vectors.

In the formula (1) the inner product is used, thus the inner product in vector space has to be defined as well. In the case of intervals, it is good to define the inner product related to selected orientation in vector space. This results from the fact that the outcome of inner product is a scalar, in other words — a value that is not an interval. If error is calculated for some value, then it will be best to relate the inner product to this value. In the case under discussion, it should be the center of the interval:

$$(A, B) = \sum_{i=1}^{n} \frac{\left(\underline{a}_i + \bar{a}_i\right)\left(\underline{b}_i + \bar{b}_i\right)}{4} \ . \tag{13}$$

The aforementioned formula satisfies all the axioms of the inner product apart from the axiom of zero value the inner product of non-zero vector with itself. Still, there are inner products that do not meet this axiom. This applies, for example, to inner product used in special relativity theory.

The calculation of direction coefficient a using the formula (1) has definite interpretation in vector space. Values x_i and y_i are the coordinates of vectors X and Y, respectively. The formula, Nermend (2009):

$$c = \frac{(X, Y)}{(X, X)} \ , \tag{14}$$

evaluates the component c of vector Y along vector X. This component informs about the scalar that could be used for the multiplication by vector X in order to make it similar to vector Y. The formula includes mean value, i.e. the value around which the graph of the coordinates of vectors X and Y fluctuates. In the case of sonar image, in order to calculate coefficient a and coefficient b of the straight line $y = ax + b$, the coordinates of vector X are treated as subsequent integer numbers from zero to $N - 1$, where N is the width of sonar image. The sequence of these numbers creates the straight line $y = x + b'$. Next, vector X is divided by the vectors: representing the constant component (X_{sr} and Y_{sr}) and representing the variable components (X_{zm} and Y_{zm}). It can be assumed that:

$$X = X_{\mathrm{sr}} + X_{\mathrm{zm}} \ . \tag{15}$$

Vector X represents the straight line $y = ax + b$, vector X_{zm} is responsible for the direction coefficient a, and vector X_{sr} for the coefficient b. For the calculation of direction coefficient, the component of vector Y_{zm} along vector X_{zm} should be determined:

$$c_{\mathrm{zm}} = \frac{(X_{\mathrm{zm}}, Y_{\mathrm{zm}})}{(X_{\mathrm{zm}}, X_{\mathrm{zm}})} \ , \tag{16}$$

and the component of vector Y_{sr} along vector X_{zm}:

$$c_{\mathrm{sr}} = \frac{(X_{\mathrm{zm}}, Y_{\mathrm{sr}})}{(X_{\mathrm{zm}}, X_{\mathrm{zm}})} \ . \tag{17}$$

The direction coefficient a is a sum of both components:

$$a = c_{\mathrm{zm}} + c_{\mathrm{sr}} \ . \tag{18}$$

For inner product defined by the expression:

$$(X, Y) = \sum_{i=1}^{n} x_i y_i \ , \tag{19}$$

in vector space in which vectors are described by the ordered n-tuples of real numbers:

$$\forall x_1, x_2, \ldots, x_n \in \mathbb{R}, X \in \mathrm{X} : X \equiv (x_1, x_2, \ldots, x_n) \ , \tag{20}$$

vectors X_{zm} and Y_{sr} are always mutually orthogonal. This means that c_{sr} always equals zero.

In vector space, where vectors are defined by intervals (10), the vector components along other vectors are regular real numbers. It is plausible to determine

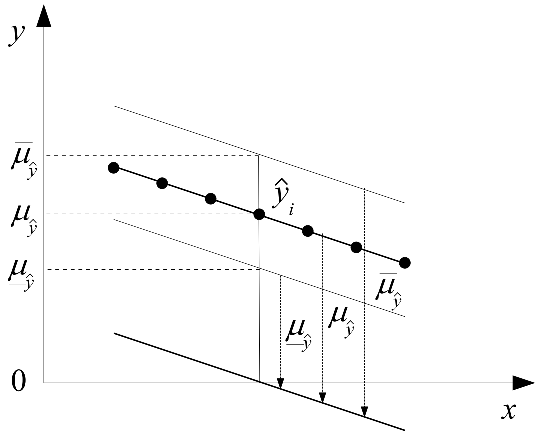

Figure 9. Obtaining the interval with zero-span

direction coefficients of the line, yet they are not defined by intervals. In order to evaluate the interval, including this coefficient, it is necessary to use a slightly different evaluation procedure.

Calculation in vector space involves using the subtraction formula different than formula used in interval arithmetic, (6):

$$\forall a, b \in \mathbb{H} : a - b \equiv \left[\underline{a} - \underline{b}; \bar{a} - \bar{b}\right] \ , \tag{21}$$

but it is conform with extended interval arithmetic.

In the case discussed, the intervals of the determined vector Y_{zm} will have the left bound equal to the right bound. This results from the fact that values $\hat{y}_i$ have a constant span of interval. Mean value $\underline{\mu}_{\hat{y}}$ will be subtracted from the straight line joining the left bounds of interval, and mean value as well as $\bar{\mu}_{\hat{y}}$ will be subtracted from the straight line joining the right bounds of interval. The intervals with zero-span are obtained in such a way (Fig. 9). Their span will be non-zero only when there is a difference between the spans of intervals for values of $\hat{y}_i$. Values c_{zm} can be considered to be exact values.

The coordinates of vector Y_{sr} belong to certain intervals. This means that the end of vector could be in any place within the hyper-cuboid, of the size determined by intervals describing the vector. In this case, the spans of all intervals are the same, thus hyper-cuboid becomes a hyper-cube (in the 2D space a hyper-cube is a square). The edges of the hyper-cube are parallel to the axes of the coordinate system. The vector described by central values of the intervals of vector Y_{sr} is perpendicular to vector X_{zm}, due to which its coordinate along vector X_{zm} equals zero. This value is determined on the basis of the formula (17). However, it is a special case.

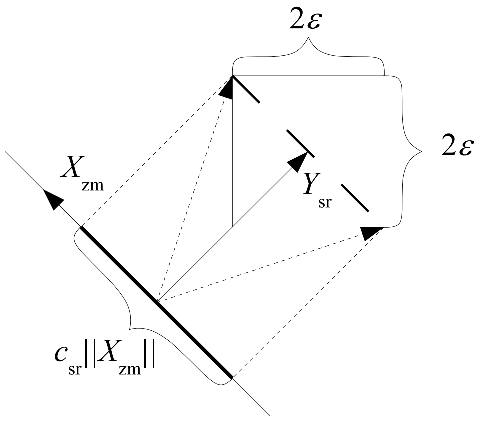

Figure 10. Component of vector Y_{sr} along vector X_{zm} in the two-dimensional space

In the case of a vector described by arbitrary values (within the intervals of vector Y_{sr}), its component along vector X_{zm} does not have to be zero. Its maximal value will be determined by two vectors described by means of the bounds of interval: the left of the first interval and the right of the second interval, as well as the right of the first interval and the left of the second interval. This is illustrated in Fig. 10. These vectors are lying on the vertices of the square connected by the diagonal. Thus, the component c_{sr} will be inside the interval:

$$c_{\text{sr}} = \left[-\frac{\sqrt{2}\epsilon}{\|X_{\text{zm}}\|}; \frac{\sqrt{2}\epsilon}{\|X_{\text{zm}}\|} \right] , \tag{22}$$

where $\|X_{\text{zm}}\|$ is the length of the vector X_{zm}.

In multi-dimensional spaces, exceeding 2D, calculation of c_{sr} becomes highly complicated. For instance, in three dimensional space, the hyper-cube becomes the cube. Because vector X_{zm} is perpendicular to vector Y_{sr} it will be lying in the plane perpendicular to vector Y_{sr}. This plane cuts the cube in such a way that the cutting surface is a regular hexagon (Fig. 11). Vector X_{zm} can have any direction and the span of interval will depend on its orientation on this regular hexagon surface c_{sr}. Two cases should be mentioned. In the first case, vector X_{zm} is parallel to one side of the regular hexagon. With such a position, the maximal plausible span of the interval is obtained. Interval c_{sr} is defined by the diagonal of cube face, and is described by the formula:

$$c_{\text{sr}} = \left[-\frac{\sqrt{2}\epsilon}{\|X_{\text{zm}}\|}; \frac{\sqrt{2}\epsilon}{\|X_{\text{zm}}\|} \right] . \tag{23}$$

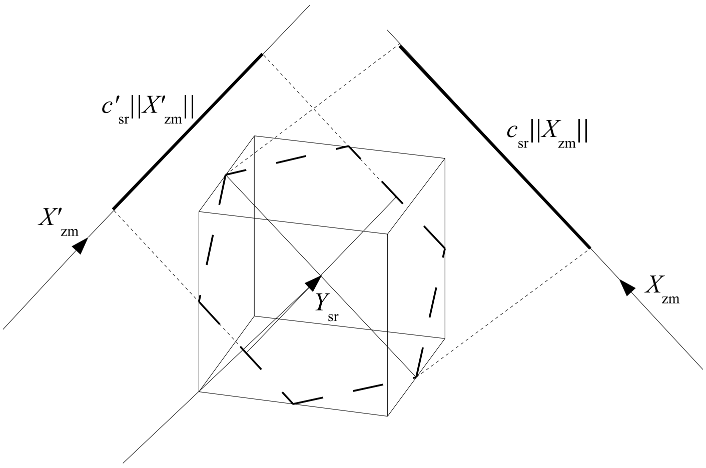

Figure 11. Component of vector Y_{sr} along vector X_{zm} in the three-dimensional space

The smallest plausible span of interval is obtained when vector X_{zm} is perpendicular to the sides of the regular hexagonal.

In four dimensional space, intersection of the hyperplane perpendicular to vector Y_{sr} with hypercube will be slightly different than in 3D space. On this hyperplane, there are the vertices of hypercube and some diagonals, just as in the case of straight line cutting the square in the 2D space. Hence, the biggest plausible interval c_{sr} will depend on the length of the diagonal:

$$c_{\mathrm{sr}} = \left[-\frac{\sqrt{4}\epsilon}{\|X_{\mathrm{zm}}\|}; \frac{\sqrt{4}\epsilon}{\|X_{\mathrm{zm}}\|}\right] . \tag{24}$$

The case of 5D space will be analogous to the 3D case. Finally, one will obtain a general form of the formula for determining the span of interval c_{sr} depending on the dimension of space. For spaces with even number of dimensions:

$$c_{\mathrm{sr}} = \left[-\frac{\sqrt{n}\epsilon}{\|X_{\mathrm{zm}}\|}; \frac{\sqrt{n}\epsilon}{\|X_{\mathrm{zm}}\|}\right] , \tag{25}$$

and for those with an odd number of dimensions:

$$c_{\mathrm{sr}} = \left[-\frac{\sqrt{n-1}\epsilon}{\|X_{\mathrm{zm}}\|}; \frac{\sqrt{n-1}\epsilon}{\|X_{\mathrm{zm}}\|}\right] . \tag{26}$$

Direction coefficient a is a sum of components c_{zm} and c_{sr} and in the case of space with an even number of dimensions it will take the following form:

$$a = \frac{\sum_{i=1}^{n} x_i \left(y_i - \mu_y\right)}{\sum_{i=1}^{n} x_i^2} \pm \frac{\sqrt{n}\epsilon}{\sqrt{\sum_{i=1}^{n} \left(x_i - \mu_x\right)^2}}, \tag{27}$$

and in space with odd number of dimensions:

$$a = \frac{\sum_{i=1}^{n} x_i \left(y_i - \mu_y\right)}{\sum_{i=1}^{n} x_i^2} \pm \frac{\sqrt{n-1}\epsilon}{\sqrt{\sum_{i=1}^{n} \left(x_i - \mu_x\right)^2}}. \tag{28}$$

Left and right bounds of the direction coefficient a can be recalculated into the value of angles, determining the left and right bounds for the angle of quay line with the horizon. With the aid of map, these values can be recalculated into the left and right bounds of the angle of sonar image with the North (azimuth).

The range of angles with the horizon determined from the sonar image of Fig. 3 is $[3.1; 13]$ degrees, and for the image in Fig. 7 it is $[6.5; 14]$.

4. Conclusion

The paper discussed the method for determining the azimuth of sector sonar image. Additionally, the range of plausible error, which is of practical importance to the creation of mosaic, requires images to have the same azimuth. The determination of the range of angles allows for comparing two images by introducing small changes into the azimuth. The method can be applied to images containing a part of quay. Yet, such a case poses a problem with erroneous indications of built-in sonar compass, resulting from the metal parts the quay. If the sonar is located far from the quay, the compass reading is precise enough, and azimuth value need not be corrected.

References

Aczel, A.D. (2000) *Statystyka w zarządzaniu* (*Statistics in Management*, in Polish). PWN, Warszawa.

Aggarwal, N. and Karl, W.C. (2006) Line Detection in Images Through Regularized Hough Transform. *IEEE Transactions on Image Processing*, **15** (3), 582–591.

Borawski, M. (2007) *Rachunek wektorowy w przetwarzaniu obrazów* (*Vector Calculus in Image Processing*, in Polish). Wydawnictwo Uczelniane Politechniki Szczecińskiej, Szczecin.

CHANTLER, M.J. and STONER, J.P. (1994) Robust classification of sector-scan sonar image sequences. *Proceedings of the Oceans Engineering for Today's Technology and Tomorrow's Preservation,* **2**, II/591 – II/596 .

KAUCHER, E. (1973) *Über metrische und algebraische Eigenschaften einiger beim numerischen Rechnen auftretender Räume*. Universität Karlsruhe, PhD thesis.

KAUCHER, E. (1980) Interval analysis in the extended interval space in computing. *Computing*, suplement, **2**, 33–49.

KOSIŃSKI, W. and PROKOPOWICZ, P. (2004) Algebra liczb rozmytych (Algebra of fuzzy numbers; in Polish), *Matematyka stosowana*, **5**, 37–63.

LANE, D.M., CHANTLER, M.J. and DAI, D. (1998) Robust tracking of multiple objects in sector-scan sonar image sequences using optical flow motion estimation. *IEEE Journal of Oceanic Engineering*, **23** (1), 31–46.

MAREŠ, M. (1989) Addition of rational fuzzy quantities: Convolutive approach. *Kybernetika*, **25**, 1–12.

MAREŠ, M. (1994)*Computation over Fuzzy Quantities*. CRC Press, Boca Raton.

MAREŠ, M. (1977) How to handle fuzzy quantities? *Kybernetika* **13**, 23–40.

MIKUSIŃSKI, J. (1953) *Operational Calculus*. Polskie Towarzystwo Matematyczne, Warszawa, in Polish.

MIKUSIŃSKI, J. (1983) *Operational Calculus*. PWN and Pergamon Press, Warszawa, Oxford.

NERMEND, K. (2009) *Vector Calculus in Regional Development Analysis*. Series: *Contributions to Economics*, Springer.

NEUMAIER, A. (1990) *Interval methods for systems of equations*. Cambridge University Press.

PERRY, S.W. and GUAN, L. (2004a) A Recurrent Neural Network for Detecting Objects in Sequences of Sector-Scan Sonar Images. *IEEE Journal of Oceanic Engineering*, **29** (3), 857–871

PERRY, S.W. and GUAN, L. (2004b) Pulse-Length-Tolerant Features and Detectors for Sector-Scan Sonar Imagery. *IEEE Journal of Oceanic Engineering*, **29** (1), 138–156

POPOVA, E. (1994) Extended interval arithmetic in ieee floating-point environment. *Interval Computations*, **4**, 100–129.

RAU, J.Y. and CHEN, L.CH. (2003) Fast Straight Lines Detection Using Hough Transform with Principal Axis Analysis. *Journal of Photogrammetry and Remote Sensing*, **8** (1), 15–34

REED, S., RUIZ, I.T., CAPUS, CH. and PETILLOT, Y. (2006) The Fusion of Large Scale Classified Side-Scan Sonar Image Mosaics. *IEEE Transactions on Image Processing*, **15** (7), 2049–2059

RUIZ, I.T., LANE D.M. and CHANTLER M.J. (1999) A Comparison of Inter-Frame Feature Measures For Robust Object Classification in Sector Scan Sonar Image Sequences. *IEEE Journal of Oceanic Engineering*, **24** (4), 458–469